

High Spatial Resolution Quantitative Imaging by Cross-calibration Using Laser Ablation Inductively Coupled Plasma Mass Spectrometry and Synchrotron Micro-X-ray Fluorescence Technique

Hao A. O. Wang^{§ab}, Daniel Grolimund^{*a}, Luc R. Van Loon^c, Kurt Barmettler^d, Camelia N. Borca^a, Beat Aeschlimann^b, and Detlef Günther^b

[§]SCS-Metrohm Foundation Award for best oral presentation

Abstract: High spatial resolution, *quantitative* chemical imaging is of importance to various scientific communities, however high spatial resolution and robust quantification are not trivial to attain at the same time. In order to achieve *microscopic* chemical imaging with enhanced quantification capabilities, the current study links the independent and complementary advantages of two micro-analytical techniques – Synchrotron Radiation-based micro X-ray Fluorescence (SR-microXRF) and Laser Ablation Inductively Coupled Plasma Mass Spectrometry (LA-ICPMS). A cross-calibration approach is established between these two techniques and validated by one experimental demonstration. In the presented test case, the diffusion pattern of trace level Cs migrating into a heterogeneous geological medium is imaged *quantitatively* with high spatial resolution. The one-dimensional line scans and the two-dimensional chemical images reveal two distinct types of geochemical domains: calcium carbonate rich domains and clay rich domains. During the diffusion, Cs shows a much higher interfacial reactivity within the clay rich domain, and turns out to be nearly non-reactive in the calcium carbonate domains. Such information obtained on the micrometer scale improves our chemical knowledge concerning reactive solute transport mechanism in heterogeneous media. Related to the chosen demonstration study, the outcome of the quantitative, microscopic chemical imaging contributes to a refined safety assessment of potential host rock materials for deep-geological nuclear waste storage repositories.

Keywords: High spatial resolution · LA-ICPMS · MicroXRF · Opalinus clay · Quantitative

Introduction

Quantitative chemical information is sought intensively in scientific research, industrial manufacture and even human life. For example, when we evaluate new materials, collect data for further simulation, guide production processes, generate quality control reports or simply watch

our daily nutrition input, quantification is definitely playing an important role. There are many analytical techniques at the *macroscopic* scale providing *quantitative* information. Specifically for elemental composition analysis, several of them are routinely utilized, for instance lab-based X-ray fluorescence (XRF), liquid-based Inductively Coupled Plasma Optical Emission Spectroscopy (ICPOES) or liquid-based ICP Mass Spectrometry (ICPMS). The lab-based XRF systems typically illuminate a probing spot much larger than a few tens of micrometers in diameter, and solution ICPOES/MS requires digestion of typically a few cubic millimeters sample prior to measurement. Consequently, all of these techniques average over a large area or volume of the sample, thus none of them is as such suitable for high spatial resolution analysis. However, as is commonly seen in nature and technology, most materials are heterogeneous and a lot of fundamental phenomena are driven by mechanisms operational at the micrometer/nanometer scale.^[1,2]

Accordingly, scientists are striving to replace the volume averaging techniques with advanced micro probing methods.^[3–5] Obviously, while pushing the limits in terms of spatial resolution, current developments are challenged towards abiding performance regarding quantification^[6,7] and sensitivity.^[8] Concerning chemical imaging, synchrotron radiation-based micro-X-ray fluorescence (SR-microXRF) analyses supersede lab-based XRF in multiple aspects, mainly due to the advantages of advanced focusing optics, high photon flux and tunable wavelength. The advanced SR-microXRF possesses the benefits of higher spatial resolution, faster data acquisition, elemental selectivity, as well as the capability for simultaneous collections of complementary chemical information such as crystallographic structure by SR-micro-X-ray diffraction (SR-microXRD)^[9] and chemical speciation by SR-micro-X-ray absorption spectroscopy (SR-microXAS).^[10,11] In contrast to the mentioned advantages, quantification of SR-microXRF images turns out

*Correspondence: Dr. D. Grolimund^a

Tel.: +41 56 310 4782

Fax: +41 56 310 4551

E-mail: daniel.grolimund@psi.ch

^amicroXAS Beamline Project

Swiss Light Source

Paul Scherrer Institut

CH-5232 Villigen PSI

^bTrace Element and Micro Analysis Group

ETH Zürich

Wolfgang-Pauli-Str. 10

CH-8093 Zürich

^cLaboratory for Waste Management

Paul Scherrer Institut

CH-5232 Villigen PSI

^dSoil Chemistry

ETH Zürich

Universitätstrasse 16

CH-8092 Zürich

to be challenging. The main reason is the lack of matrix-matched standards. Prepared by routine grinding methods and compressed into pellets, such matrix-matched materials do not reach sufficient homogeneity on the sub-micrometer level. This, however, is a critical prerequisite for calibration of high spatial resolution techniques based on micro/nano beams. An alternative approach of quantification is to perform full spectra analysis for each pixel based on fundamental parameters using standard-free or non-matrix matched standard methods. Within this approach, the accuracy of quantification is critically dependent not only on the accurate knowledge of the average composition and density of each voxel, but even on the chemical gradients within each probing volume (stratification). Further, limited counting statistics may restrict quantification of trace elements. Consequently, until recently, most imaging applications based on SR-microXRF were semi-quantitative or qualitative representations.

Laser Ablation Inductively Coupled Plasma Mass Spectrometry (LA-ICPMS) was introduced in the mid 80s by Gray^[12] as a versatile quantitative technique. Up to now, researchers benefit from its large dynamic range, allowing major, minor, trace and even ultra trace elements quantification, yet still providing moderate spatial resolution by focused laser beams. Various types of mass analyzers are popular for specific purposes. Quadrupole is a low cost, sensitive, four-rod based analyzer. During one integration time, ions with one mass-to-charge ratio (M/Z) are flying along a certain trajectory exclusively and are collected by an electron multiplier detector. Quadrupole MS has adequate m/z resolution for most of the routine analyses, hence, currently occupying most of the labs. Other more advanced mass analyzers include double-focusing sector-field type mass spectrometers for improved sensitivity and higher M/Z resolution measurements, or time-of-flight type for semi-simultaneous full mass spectrum acquisition. Different laser sources ranging from UV to IR wavelength and from femto- to nano-second pulse are currently employed in nearly routine operations. A detailed comparison and discussion of the different laser systems employed in LA-ICPMS can be found elsewhere.^[13–15]

In this study, we will show the capability of cross-calibrating *qualitative* high spatial resolution SR-microXRF analysis by corresponding *quantitative* LA-ICPMS results from the same probing area, and finally generate full *quantitative* chemical images with high spatial resolution. To demonstrate this approach, a case study related to contaminant migration in the subsurface is presented. The distribution

pattern of a trace pollutant diffusing into a heterogeneous geological medium is imaged. As a potential host rock for nuclear waste repositories, sedimentary clay rocks (e.g. Opalinus clay rock in Switzerland^[16]) have attracted much attention from the nuclear waste management community. Various *macroscopic* measurements have been conducted revealing lumped physical and chemical properties such as sorption affinities, diffusion coefficients, porosities, etc. However such *macroscopic* investigations average over a large volume and provide therefore only an 'empirical' description of states of the entire system. As pointed out before, many mechanisms or fundamental processes are operational on the *microscopic* level. In order to gain an adequate understanding about the fundamental processes defining the evolution of the entire system, one must gather knowledge on the corresponding *microscopic* and *nanoscopic* scale. Along these lines, our effort shall complement the *macroscopic* description of states with *quantitative* chemical, process relevant information on the *microscopic* level.

Experimental Details

Sample

We demonstrate our cross-calibration approach in a test case study of imaging trace isotope distribution in a heterogeneous medium (Opalinus clay rock). The sample material originates from a field-scale migration experiment conducted at the Mont Terri Underground Rock Laboratory (located in the north-western part of Switzerland).^[17,18] In this experiment, a borehole was first drilled into the Opalinus clay rock formation, followed by an injection and recirculation of a multi-isotope tracer solution. During nine months, trace isotopes migrated radially from the injection hole into the sedimentary rock. At the end of the field experiment, an overcore was excavated.^[17] Our sample was obtained from an experimental core, which was extracted out of the overcore perpendicular to the injection borehole. The sample was further sectioned along the diffusion direction by a diamond saw. We focused our study on the migration pattern of stable ¹³³Cs, which was used as chemical analogue of the radioactive Cs isotopes present in nuclear waste. Preliminary microXRF measurements on cross-sections showed a characteristic heterogeneity with two types of distinctive domains.^[11] This geochemical heterogeneity shows a typical correlation length of a few hundreds of micrometers. Based on XRD measurements, the two domains were identified to be either calcium carbonate rich domains or clay minerals dominated

domains. A compilation of geochemical information related to the Opalinus clay formation at Mont Terri is reported elsewhere.^[19]

Instrumental Setups

Both one-dimensional (1D) and two-dimensional (2D) chemical images were recorded by *quantitative* LA-ICPMS and high spatial resolution *qualitative* SR-microXRF consecutively. Obviously, the non-destructive XRF analysis should be followed by the destructive ablation technique. However, within the framework of this pilot study, the destructive LA was done first, leaving a microscopic topological trace simplifying the spatial alignment of the two probing areas. 1D and 2D traces remaining after LA scans are shown in Fig. 1a and 1b. To ablate the clay rock material, we operated a 193 nm wavelength ArF excimer laser system (Lambda Physik, Goettingen, Germany) at 23.6 J/cm² fluence. Laser spot size was 10 μm for both types of measurements. During the line scan, the laser was running at 10 Hz ablation frequency with a sample feed rate of 15 $\mu\text{m/s}$. In case of the area scan, the image was stitched from 64 sub-area-scans, each of which was a 5 \times 5 LA matrix raster. In one pixel, five laser shots at 10 Hz were fired without sample feed before translating 20 μm to the next ablation (pixel) location. The settling time between two pixels was 3 s, mainly taking into account the 1–2 s washout time of the LA cell. A description of the used LA cell can be found elsewhere.^[20] The Agilent 7500cs ICP-quadrupole-MS (Agilent Technologies, Waldbronn, Germany) was operated at a power of 1500 W and in peak hopping mode. Sequentially, each isotope was collected for 50 ms in the case of line scan and a reduced integration time of 5 ms was used during the area scan. In total, 10 isotopes including the trace Cs, major and minor matrix elements were measured. A 1.5 m long poly(tetrafluoroethylene) (PTFE) tubing transported the LA generated aerosol to the ICPMS using a helium carrier gas flow of 1 L/min. Argon at a flow rate of 0.85 L/min was mixed with the He carrier gas and aerosol in a glass mixing bulb right before entering the plasma torch. A NIST610 glass standard reference material was employed as an external calibration standard. The use of this non-matrix-matched standard was validated based on calibrations using compressed Opalinus clay pellets with known Cs concentrations. The validation showed an agreement within 10%, in case of appropriate total mass normalization.^[21]

SR-microXRF measurements were conducted at the microXAS beamline operational at the Swiss Light Source (SLS), Paul Scherrer Institut, Villigen,

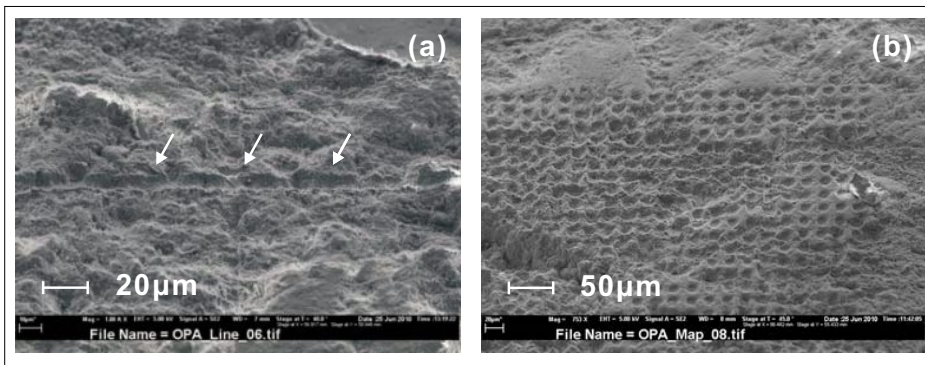


Fig. 1. Scanning electron microscopy (SEM) images of the topological traces introduced by the laser ablation process. Shown are the marks after a 1D line scan (a) and a 2D matrix scan (b).

Switzerland. Monochromatic insertion device radiation with a photon energy of 7.1 keV was obtained by the usage of a double-crystal monochromator equipped with a pair of Si(111) crystals. The monochromatic beam was further collimated by slits and focused by a Kirkpatrick-Baez mirror system into a $3 \times 3 \mu\text{m}^2$ square illumination. One-dimensional and two-dimensional chemical images were obtained by x-y rastering of the sample against the spatially fixed micro beam. The scanning in the primary scan direction (x) was conducted in on-the-fly mode providing average compositional information independent of pixel size. The fluorescent emissions from the sample were collected simultaneously by two different types of detectors: i) an energy dispersive X-ray spectrometer (EDX, Si drift diode system, KETEK) for major and minor matrix element acquisition; ii) a Microspec wavelength dispersive X-ray spectrometer (WDX) for trace Cs signal collection. The WDX as a detector system with an energy resolution of a few electron volts is mandatory to discriminate the Cs emission from potential interferences of Ca $K\beta$ on the low energy side as well as Ti $K\alpha$ on the high energy side. The 1D line scan speed was constant at $1.25 \mu\text{m/s}$, which resulted in a pixel size of $2.5 \mu\text{m}$. For the 2D area scan, a pixel size of $3 \times 3 \mu\text{m}^2$ was chosen.

Data Evaluation

An approximately 30 mm line along the Cs diffusion direction was measured by both techniques. In case of LA-ICPMS, each data point was corrected due to the slow washout of the ablation cell assuming an exponential signal decay manner.^[22] This deconvolution procedure served the purpose of diminishing the influence of previous ablation shots to the actual reading. Due to different advancing step sizes, the LA line scan data set consisted of three-fold less data points as compared to SR-microXRF over the same distance. In order to match the spatial resolution for subsequent comparison, the two sig-

nal traces were moving averaged, in a way that the distance of the averaging window was about the same distance for both data sets. The averaged distance was chosen to be in the same range as the geochemical micro heterogeneity. Prior to comparison by correlation plots, the averaged XRF line scan data were interpolated to the spatial grid of the LA measurement. Since the two techniques were not perfectly aligned, mismatches at the boundaries between clay rich and calcium carbonate rich domains prevent a direct correlation from the whole distance range. Therefore, both Cs line scans were filtered based on a criteria that LA Ca concentration $<10\%$ and XRF Ca count rate <4000 counts per second (cps), assuring that the Cs data points included in the correlation map are all from the clay rich domain. The scattered plot with reduced Cs data points was described and summarized in a box chart representation. Each box was calculated from one of the equally spaced sections of the filtered Cs LA data points, from 0 to $240 \mu\text{g/g}$ with a step size of $30 \mu\text{g/g}$.

Concerning two-dimensional chemical imaging, the independent measurements by LA-ICPMS and SR-microXRF were conducted in two different analytical facil-

ities using completely different coordinate systems during 2D scanning. In order to match the orientation of displayed images, the original 2D data were aligned by using rotation transformation and correcting spatial distortion.

Results and Discussion

Line Scan

Fig. 2 illustrates the chemical composition in the direction of the Cs migration measured by the two independent micro-analytical techniques LA-ICPMS and SR-microXRF. These 1D line scans cover the whole range from the injection borehole/clay rock interface into the pristine Opalinus clay rock. The *quantitative* LA-ICPMS result demonstrates a Cs distribution pattern, which correspond to an almost ideal diffusion profile (Fig. 2a). Close to the interface, the Cs concentration is elevated up to $\sim 200 \mu\text{g/g}$ and remains nearly constant in the first few millimeters away from the inlet. At further distances, a typical diffusion front with gradually decreasing Cs concentration is established. After this decrease of nearly two orders of magnitudes, the Cs concentration reaches the geological background level of $\sim 6 \mu\text{g/g}$. Fig. 2c shows the corresponding *qualitative* SR-microXRF Cs line scan. By comparing to the LA profile (Fig. 2a), the concord concerning profile shape is readily confirmed. In contrast to the LA data, the XRF signal obtained with the WDX spectrometer setup from within the geological background region is close to the limit of detection. On the other hand, however, the SR-microXRF recorded profile comprises a higher spatial resolution. It is important to point out here, that in contrast to an ideal diffusion pattern, both independent measurements include, consistently, several characteristic glitches of reduced local Cs concentrations.

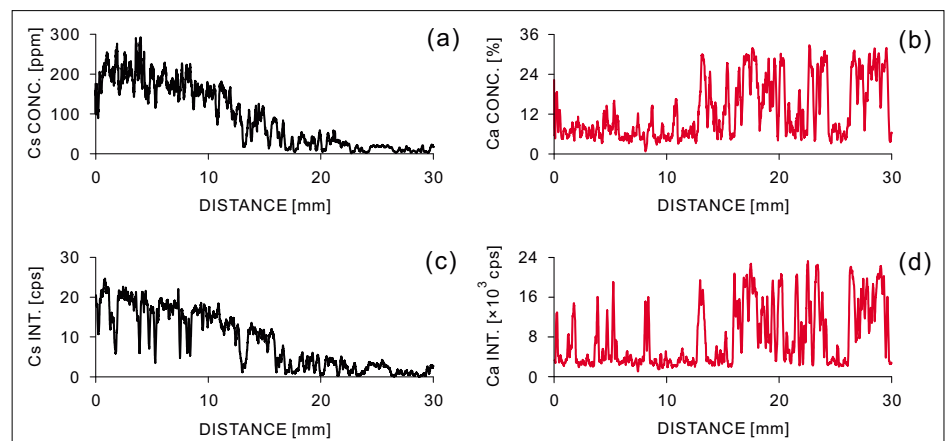


Fig. 2. Comparison of a Cs diffusion profile measured as line scan by LA-ICPMS (a) and SR-microXRF (c). The corresponding line scan measurements of the matrix element Ca are depicted for the two analytical techniques in (b) and (d).

Corresponding to the Cs line scans, the profiles of the major matrix component Ca are shown in Fig. 2b (LA-ICPMS) and Fig. 2d (SR-microXRF). Again, both types of measurements are in close agreement. Several corresponding characteristic mesa and trenches are immediately recognized. The Ca signals represent two distinct populations, high Ca concentration domains and low Ca concentration domains. Each individual domain extends over tens to hundreds of micrometers. Within each domain the Ca concentration remains rather constant. However, at the boundaries, the two types of domains are sharply separated with remarkable Ca gradients within a narrow boundary region. Over only a few micrometers, the Ca concentration is changing by more than one order of magnitude. This characteristic spatial distribution pattern corresponds to a reproduction of the geochemical heterogeneity present in the investigated sedimentary rock material.

The aforementioned glitches in the Cs diffusion profile turn out to be spatially correlated to the domains of elevated Ca concentration. This anti-correlation between Ca and Cs expresses itself along the entire scanned line, for both techniques independently and consistently. Consequently, the observed strong modulation of the trace element signals and matrix composition are due to the geological micro-heterogeneity of the sedimentary rock, and are certainly not artefacts or noise contributions within the present measurements.

Even though the general pattern for both, the trace element Cs and the major matrix element Ca obtained by the two independent analytical methods, match well, a closer inspection reveals minor differences locally. Deficits in sample aligning precision across the two analytical setups contribute mostly to these specific variations. The independent measurements by LA-ICPMS and SR-microXRF were conducted in two different analytical facilities using completely different coordinate systems during scanning. Despite best efforts, the estimated spatial displacement of the two traces is about 20 μm over the entire scan range of 30'000 μm . In relation to the micrometer spot sizes of the used micro-analytical techniques and in view of the geochemical domain sizes, such misalignment is definitely of influence. The impact of misalignment is expected to be most spurious near domain boundaries. Another potential explanation for the local differences is the different probing depth of LA and XRF analysis. In LA, the 10 μm laser spot removed only ~ 3 μm micrometers deep material on the sample surface. On the other hand, the (element specific) XRF probing volume (defined by excitation beam penetration depth

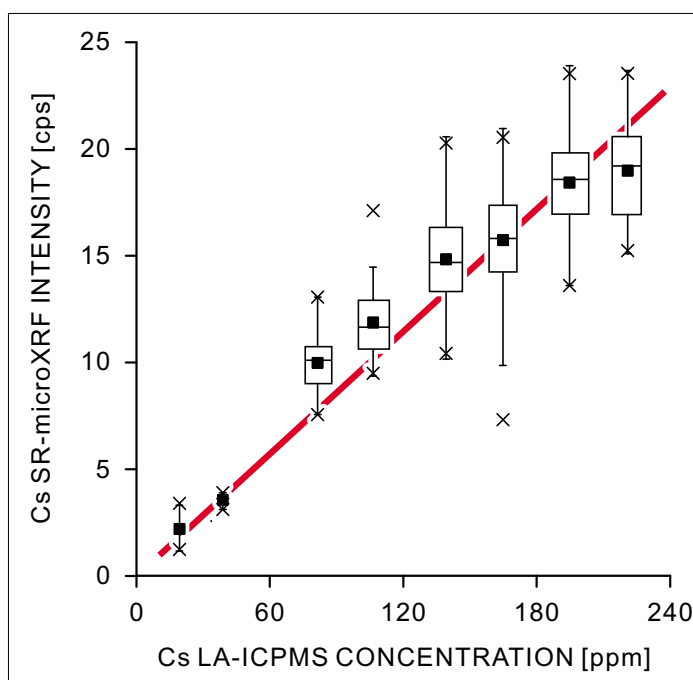


Fig. 3. Box chart plot of the correlation map for Cs between SR-microXRF and LA-ICPMS. Box width and height indicate the 25 and 75 percentiles of the data points in both dimensions. The black solid squares represent the mean value positions, the horizontal lines the median values in the y dimension. Whiskers are used to define the inner fences for outliers. The upper and lower crosses mark the 1 and 99 percentiles, respectively. A linear regression of the data is depicted as red line.

and fluorescence radiation escape length) extends about one order of magnitude deeper into the sample to at least 30 μm . As for the effect of beam offset, in particular at domain boundaries, the disk-like LA voxel and rod-like micro-XRF voxel can potentially probe different average voxel compositions.

Cross-calibration Approach

As can be recognized from Fig. 2a and 2c, the nearly ideal 1D Cs diffusion profile is covering one to two orders of magnitude in Cs concentration. This allows the generation of a robust Cs calibration curve, providing a tool to quantify the *qualitative*, but high spatial resolution XRF image. Fig. 3 depicts the box chart plot of such a cross-calibration between the two independent micro probing techniques. Details about the statistical figures represented by the boxes can be found in the figure caption. In total, the eight sections cover almost the whole concentration range indicating a clear correlation. In the first two sections, raw data points are narrowly distributed, so that the statistical box representations are omitted. The outcome of a linear regression (red line) attests the clear correlation. Based on such a robust cross-calibration, multi-dimensional qualitative Cs SR-microXRF mappings can be transformed into high resolution quantitative chemical images (Fig. 4).

Obviously, the presented Cs calibration curve corresponds to a rather special case. The fine gradient of the calibration curve could only be accomplished based on the extended range and localized Cs diffusion front present in our system. For most major and minor matrix elements present in the heterogeneous medium, such distinct

chemical gradients extending over multiples of the used beam sizes can not be observed. As a consequence, the number of possible pairs of values for calibration is limited to the number of domains with different concentration levels. As a practical example, in the present case study the cross-calibration for Ca had to be based on only two pairs of values derived from the two distinct domains of low and high Ca concentrations.

Two-dimensional Imaging

Close to the inlet region with high Cs concentration an area of $800 \times 800 \mu\text{m}^2$ on the cross-section of the Opalinus clay sample was imaged by LA-ICPMS and SR-microXRF. Analogous to the line scan, for the reason of easier imaging alignment, LA analysis was conducted prior to SR-microXRF imaging. The imprint of the 40×40 LA matrix is pictured in Fig. 1b. As apparent from this figure, the chosen laser spot size of 10 μm did not fully cover the pixel area. This data sampling strategy was given preference for the following reasons. First, the considerable settling time due to slow washout time did not allow for a significant larger number of total pixels. Second, the spatial instability of subsequent laser shots results in a slight jitter concerning ablation crater sizes. Finally, the definite spacing between ablation locations decreased the potential risk of uptake of deposited aerosol around the craters. However, the spatially moderately resolved LA image does still show the characteristic features of the elemental distributions as observed by microXRF. Yet, for a better comparison of the images obtained by the two techniques, the original LA images were 2D-interpolated to match

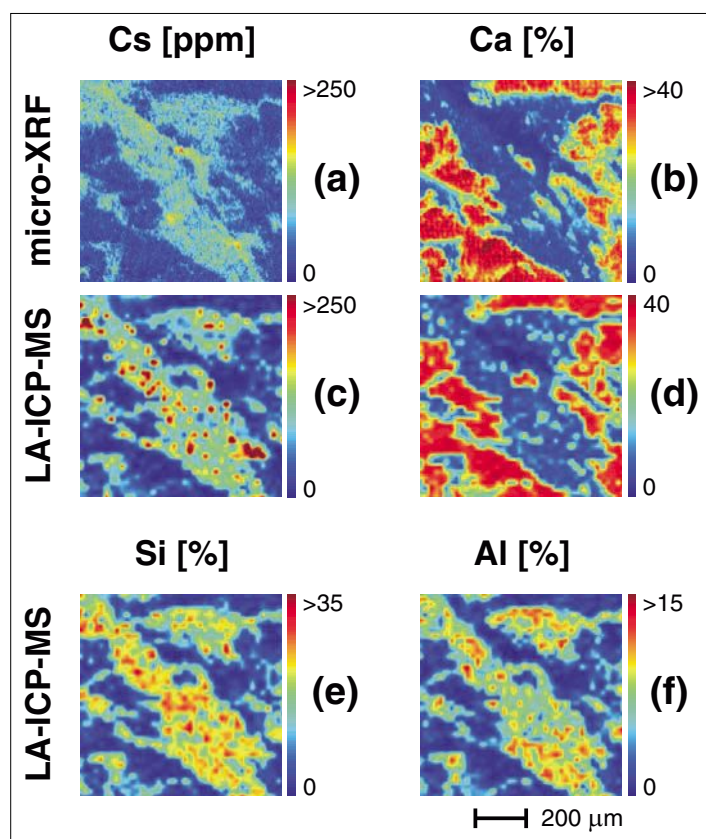


Fig. 4. Comparison of two-dimensional chemical images recorded by SR-microXRF (a,b) and LA-ICPMS (c,d) for Cs and Ca, respectively. LA-ICPMS measurement for Si and Al are illustrated in (e) and (f).

the resolution of the SR-microXRF measurements.

Inspecting the Cs distribution pattern (Fig. 4a and 4c), high Cs concentration domains and low Cs concentration domains are immediately recognized. In general, the two independent methods yield corresponding Cs distribution pattern, except for apparently more pronounced Cs 'hot spots' observed in LA. The high resolution SR-microXRF data indicate the presence of tiny, micron-sized local enrichments of Cs. These hot spots are represented as single pixels in the XRF image, while the 2D-interpolation of the coarser LA image is responsible for the observed blurring artifact. The high spatial resolution SR-microXRF image (Fig. 4a) was quantified on the basis of the cross-calibration curve discussed before. Overall, the averaged Cs concentrations are in close agreement between the two images, representing a convincing validation of the cross-calibration approach.

Fig. 4b and 4d show a comparison of the Ca distribution recorded by both techniques. The two chemical images show a close correspondence. The two-domain nature of the Opalinus clay rock as proposed based on the line scan is unequivocally evidenced in the 2D images. Sharp boundaries between domains are readily seen. Both techniques reveal a remarkable homogeneity of the Ca levels within the different geochemical domains. Due to the higher spatial resolution of the qualitative SR-microXRF Ca image distinct features

such as changes at the domain boundaries and micro heterogeneities within the domains are better resolved. Worth addressing is the dotted pattern observable at the bottom left part of the XRF image. The periodic modulations in the Ca intensities are consistent with the pattern of the LA craters (Fig. 1b) and can be attributed to the topological surface roughness introduced by the laser ablation process. Such quantification artefacts due to a sample surface roughness larger than the size of the used micro-beam correspond to potential shortcomings of quantitative SR-microXRF analysis.

From the correlated LA and XRF Ca maps, two anchor areas of low and high Ca concentrations were selected from within well delineated domains and used to calculate a cross-calibration curve. The high spatial resolution *quantitative* chemical image of the matrix element Ca could be generated accordingly (Fig. 4b).

In the case of the investigated geological sample, Si and Al are typical indicator elements of clay minerals. However, the routine operation mode of the microXAS hard X-ray microprobe facility (*e.g.* operation at ambient air, use of detector windows, high energy of excitation beam, *etc.*) limits the sensitivity towards these low Z elements considerably. Special measures would have to be taken (such as He-bagging) to obtain robust measurements. Opposite, concerning isotope sensitivity, LA-ICPMS does not show such a systematic Z dependence and is capable in analyzing these geologi-

cally relevant matrix elements. As depicted in Fig. 4e and 4f, Si and Al are observed concerted in the same domains. These clay rich regions correspond to the well-separated counterparts of the Ca rich (calcite) domains. The local concentrations of Si and Al vary considerably, but for these two elements no obvious correlation (except the coexistence in the same domain) can be identified. This observation represents an indicator for a complex mixture of multiple mineral components existing in the clay rich domain.

Inspecting the distribution pattern of the trace contaminant Cs in comparison with the chemical images of the different matrix elements, the correlation between Cs and clay, as well as the anti-correlation between Cs and Ca is definitive. The reactive transport pattern of Cs represents a clear effigy of the clay distribution. The obtained chemical images document convincingly the profound impact of chemical micro-heterogeneity regarding local reactivity and consequently reactive solute transport.

Conclusions

A novel cross-calibration approach based on independent micro-analytical techniques is described in this work. This method combines the complementary advantages of LA-ICPMS and SR-microXRF and yields high spatial resolution *quantitative* chemical images of major, minor and trace elements. To validate this approach, the trace element Cs and several major matrix elements in a Cs-infiltrated Opalinus clay rock sample were analyzed by both methods and cross-calibrated. A close correlation between the results obtained by the two techniques can be established validating the appropriateness and robustness of the applied cross-calibration approach.

Quantitative information can be extracted from the 1D (line scans) and 2D (maps) chemical images allowing to identify chemical processes, specify mass balances and to calculate corresponding reaction rates. In the present application, a pronounced geochemical micro-heterogeneity of the Opalinus clay rock was documented. Moreover, the quantitative chemical images evidenced the defining impact of this micro-scale heterogeneity on reactive transport processes. Such findings can be expected to contribute to an advanced understanding of the basic reactive transport mechanism and consequently lead to an improved reliability of safety assessments or to more efficient remediation strategies.

Despite the promising results obtained, for both techniques limitations regard-

ing high resolution quantitative chemical imaging have still to be considered. In case of LA-ICPMS, the moderate data acquisition speed mainly due to the large dispersion of the analytical instrumentation represents an inconvenient restriction. Concerning SR-microXRF, quantification remains a considerable challenge. Despite recent progress towards full spectra recording and analysis based on standard-free fundamental parameter concepts, in particular in case of micro-structured matrixes dominated by low Z elements, the uncertainty regarding local matrix composition results in limited confidence intervals. Obviously, numerous ongoing developments in various fields of analytical chemistry will contribute to diminish these limitations. Concurrently, the complementary use of independent micro-analytical techniques results in improved quantitative chemical imaging.

Acknowledgements

We would like to thank Paul Wersin and Olivier Leupin, scientific program managers affiliated with the Mont Terri Underground Rock laboratory, for providing sample material. Julien Zimmermann is acknowledged for his expertise and support regarding the SEM work. The synchrotron based measurements were performed at the microXAS beamline of

the Swiss Light Source, Paul Scherrer Institut, Villigen, Switzerland. Financial support by Swiss National Foundation (SNF) is acknowledged (project 200021-119779).

Received: January 24, 2012

- [1] A. Bogdan, M. J. Molina, H. Tenhu, E. Mayer, E. Bertel, T. Loerting, *J. Phys.: Cond. Mat.* **2011**, 23, 035103.
- [2] Q. Yu, Z.-W. Shan, J. Li, X. Huang, L. Xiao, J. Sun, E. Ma, *Nature* **2010**, 463, 335.
- [3] H. Mimura, S. Handa, T. Kimura, H. Yumoto, D. Yamakawa, H. Yokoyama, S. Matsuyama, K. Inagaki, K. Yamamura, Y. Sano, K. Tamasaku, Y. Nishino, M. Yabashi, T. Ishikawa, K. Yamauchi, *Nat. Phys.* **2010**, 6, 122.
- [4] O. L. Krivanek, M. F. Chisholm, V. Nicolosi, T. J. Pennycook, G. J. Corbin, N. Dellby, M. F. Murfitt, C. S. Own, Z. S. Szilagy, M. P. Oxley, S. T. Pantelides, S. J. Pennycook, *Nature* **2010**, 464, 571.
- [5] S. Haessler, J. Caillat, W. Boutu, C. Giovanetti-Teixeira, T. Ruchon, T. Auguste, Z. Diveki, P. Breger, A. Maquet, B. Carre, R. Taieb, P. Salieres, *Nat. Phys.* **2010**, 6, 200.
- [6] H.-J. Wang, M. Wang, B. Wang, X.-Y. Meng, Y. Wang, M. Li, W.-Y. Feng, Y.-L. Zhao, Z.-F. Chai, *J. Anal. Atom. Spectrom.* **2010**, 25, 328.
- [7] J. S. Becker, R. C. Dietrich, A. Matusch, D. Pozebon, V. L. Dressler, *Spectrochim. Acta B* **2008**, 63, 1248.
- [8] C. Latkoczy, D. Günther, *J. Anal. Atom. Spectrom.* **2002**, 17, 1264.
- [9] E. Nakazawa, T. Ikemoto, A. Hokura, Y. Terada, T. Kunito, S. Tanabe, I. Nakai, *Metallomics* **2011**, 3, 719.
- [10] D. Grolimund, M. Senn, M. Trottmann, M. Janousch, I. Bonhoure, A. M. Scheidegger, M. Marcus, *Spectrochim. Acta B* **2004**, 59, 1627.
- [11] H. A. O. Wang, D. Grolimund, L. R. Van Loon, K. Barmettler, C. N. Borca, B. Aeschlimann, D. Günther, *Anal. Chem.* **2011**, 83, 6259.
- [12] A. L. Gray, *Analyst* **1985**, 551
- [13] M. Guillon, I. Horn, D. Günther, *J. Anal. Atom. Spectrom.* **2003**, 18, 1224.
- [14] J. Gonzalez, X. L. Mao, J. Roy, S. S. Mao, R. E. Russo, *J. Anal. Atom. Spectrom.* **2002**, 17, 1108.
- [15] F. Poitrasson, X. Mao, S. S. Mao, R. Freydiser, R. E. Russo, *Anal. Chem.* **2003**, 75, 6184.
- [16] Nagra (Wettingen, Switzerland; <http://www.nagra.ch>), Project Opalinus clay. Safety report: Demonstration of disposal feasibility for spent fuel, vitrified high-level waste and long-lived intermediate-level waste (Entsorgungsnachweis). Nagra Technical Report NTB 02-05 **2002**.
- [17] P. Wersin, L. R. Van Loon, J. M. Soler, A. Yllera, J. Eikenberg, T. Gimmi, P. Hernán, J. Y. Boisson, *Appl. Clay. Sci.* **2004**, 26, 123.
- [18] A. Möri, L. Inderbitzin, C. Nussbaum, J. Eikenberg, M. Rütthi, C. Aubry, N. Brisset, H. Steiger, P. Bossart, Mont Terri Project, Technical Note 20 **2003**.
- [19] M. H. Bradbury, B. Baeyens, *Geochim. Cosmochim. Ac.* **1998**, 62, 783.
- [20] M. B. Fricker, D. Kutscher, B. Aeschlimann, J. Frommer, R. Dietiker, J. Bettmer, D. Günther, *Int. J. Mass Spectrom.* **2011**, 307, 39.
- [21] M. Guillon, K. Hametner, E. Reusser, S. A. Wilson, D. Günther, *Geostand. Geoanal. Res.* **2005**, 29, 315.
- [22] D. Bleiner, D. Günther, *J. Anal. Atom. Spectrom.* **2001**, 16, 449.